JOURNAL OF APPLIED ELECTROCHEMISTRY 19 (1989) 174–182

Evaluation of mass transport in copper and zinc electrodeposition using tracer methods

H. M. WANG, S. F. CHEN, T. J. O'KEEFE

University of Missouri-Rolla, Materials Research Center and Department of Metallurgical Engineering, Rolla, MO 65401, USA

M. DEGREZ, R. WINAND

Université Libre de Bruxelles, Department Metallurgy–Electrochemistry, CP 165, 50, avenue F.D. Roosevelt, B 1050 Brussels, Belgium

Received 14 July 1988; revised 6 November 1988

Control of the electrocrystallization process is essential in the deposition of metals from aqueous electrolytes. A knowledge of the influence of mass transfer on the metal ion reduction is a critical element in any number of electrolytic processes, particularly where relatively high current densities are desired. The use of more positive ion tracer techniques as a means of experimentally determining some of the mass transport properties of interest are described. Examples for copper, zinc and zinc alloys electrolysis are included.

Nomenclature

C_b	concentration in the bulk of the solution
C_s	concentration at the surface of the electrode
d	hydraulic diameter of the cross section of the cell
D	diffusion coefficient
e_{Me}	equivalent weight of Me
F	Faraday number
g	acceleration due to gravity
Gr	Grashof number
H	hydrodynamic entrance length
(It)	quantity of electricity (current times time)
J	current density
J_{dl}	diffusion limiting current density
$k = J_{dl}/zFC$	mass transfer coefficient
L	electrode length
P_{Me}	deposited mass of Me
$Re = vd/\nu$	Reynolds number
$Sc = \nu/D$	Schmidt number
Sh	Sherwood number
v	speed of electrolyte
z	number of electrons exchanged in the electrode reaction
δ	thickness of the diffusion layer
η_d	diffusion overvoltage
ν	kinematic viscosity of electrolyte
ϱ	average density across diffusion layer
ϱ_b	bulk electrolyte density
ϱ_i	density of the electrolyte at the surface of the electrode
ω	rotation speed of the electrode

1. Introduction

The structure and morphology of electrodeposited metals continues to be one of the main concerns in industrial operations. The physical nature of the deposit can influence not only the functional properties, but also the chemical analysis. Two parameters which play a major role in electrocrystallization and structure determination are mass transport and inhibition effects.

One way of representing the relationship between these two parameters is through the use of fields of predominance for the main types of electrolytic deposits introduced by Fischer [1] and shown by the diagram [2–4] in Fig. 1 where: mass transport is represented by the ratio of the current density J to the diffusion limiting current density J_{dl}; inhibition is increased due to the presence at the electrode surface of substances (molecules, atoms, ions) different from the depositing metal which are physically or chemically adsorbed.

It was shown [5] that in a pure acid copper sulfate solution, transition from FT to UD type occurs at a constant value of the ratio J/J_{dl} (approximately 0.35) independently of the electrolyte flow rate. This shows the direct influence of mass transfer on the structure of cathode deposits and also the way to increase productivity without changing the properties of the deposits.

Other recent theoretical and applied studies [6, 7], ranging from bench scale to full size pilot cells, have also shown the importance of enhanced mass transfer

0021-891X/89 $03.00 + .12

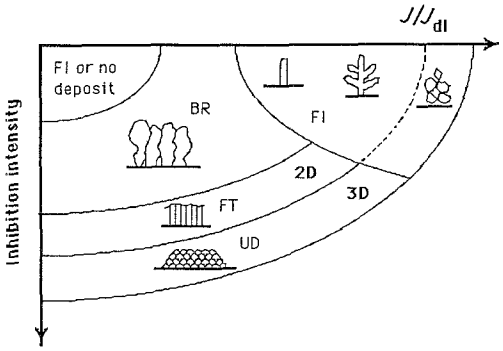

Fig. 1. Main types of electrodeposits as a function of mass transfer rate and inhibition intensity. FI: field oriented, isolated crystals type (whiskers, dendrites or loose crystalline powder); BR: basis reproduction type (coherent deposits: grain size and surface roughness increase with deposit thickness); FT: field oriented texture type (coherent deposits; grain size almost constant throughout the deposit thickness; rather low surface roughness); UD: unoriented disperser type (coherent deposits; small grain size; new crystals generated throughout deposit thickness); 2D: bidimensional nucleation; 3D: tridimensional nucleation.

in improving the performance of many electrolytic systems.

The field of continuous high current density plating of zinc on steel sheet has been particularly active during the past decade resulting in the construction and operation of new facilities worldwide [8]. High current density electrorefining of copper is also promising [9].

In this paper, a brief description of tracer methods for mass transfer measurements in electrodeposition is given. Examples of the utilization of these techniques for copper and zinc deposition is also presented.

2. Theoretical considerations

When a cation Me^{z+} is consumed at a cathode, its concentration falls from C_b in the bulk of the solution to a value C_s at the surface of the electrode through the diffusion layer δ. For a diffusion coefficient of D, when enough supporting electrolyte is present in order to suppress the migration contribution, the diffusion limiting current density is

$$J_{dl} = zF\frac{D}{\delta}C_b \qquad (1)$$

where δ is a function of the electrolyte flow conditions. Accordingly, electrolysis occurring at a current density J, lower than J_{dl}, results in a diffusion overvoltage

$$\eta_d = \frac{RT}{zF}\ln\left(1 - \frac{J}{J_{dl}}\right) \qquad (2)$$

Various methods may be considered to characterize mass transfer to the electrode. One is the direct measurement of the diffusion limiting current density. In this method, a cathodic polarization curve is drawn and J_{dl} is obtained when a sudden increase in cathodic overvoltage appears while the current density remains constant. However, for high Me^{z+} concentrations in agitated solutions, at values approaching 60% of J_{dl}, the amount of electricity passed through the cell is so high that enough metal has been deposited at the cathode to achieve a significant and continuous increase in roughness of the electrode, resulting in erratic results.

Interferometric measurements [13–17], based on variations of refraction index due to concentration gradient in the diffusion layer, and the freezing method [18], have been used but are rather complicated.

The method chosen for this paper is the tracer method [19–22]. Its basic principle is as follows. A small concentration of a 'soluble' tracer ion is added to the electrolyte; it must plate at a more positive potential than the studied metal and be deposited at the cathode at its own diffusion limiting current density, $J_{dl\,tracer}$, during the deposition of the studied metal Me. Codepositing Me and the tracer at a given current density and for a given quantity of electricity $(It)_{total}$ results, after chemical analysis, in

$$(It)_{tracer} = P_{tracer}F/e_{tracer} \qquad (3)$$

where $(It)_{tracer}$ is the quantity of electricity used to deposit the analysed mass of tracer P_{tracer}.
Accordingly,

$$J_{dl\,tracer} = J\frac{(It)_{tracer}}{(It)_{total}} = F\frac{D_{tracer}}{\delta_{total}}C_{b\,tracer}z_{tracer} \qquad (4)$$

In order to be able to obtain the diffusion limiting current density of the metal $J_{dl\,Me}$ it should be noted that δ is a function of D.

According to Pickett and Ong [23], the Chilton–Colburn Equation 5 is verified in a fully developed forced turbulent flow in a channel cell:

$$Sh \propto Re^{0.8}Sc^{1/3} \qquad (5)$$

where $Sh = 10^{-3}J_{dl}d/zFCD$ is the Sherwood number characterizing mass transfer to the electrode with d in cm, J_{dl} in mA cm^{-2}, F in As mole^{-1}, C in mole cm^{-3} and D in cm^2 s^{-1}.

Accordingly, if Re is constant, $Sh \propto (v/D)^{1/3}$ and $J_{dl} \propto zFCDSh/d$, thus:

$$J_{dl\,Me} = \frac{z_{Me^{z+}}}{z_{tracer}}J_{dl\,tracer}\frac{C_{b\,Me^{z+}}}{C_{b\,tracer}}\left(\frac{D_{Me^{z+}}}{D_{tracer}}\right)^{2/3} \qquad (6)$$

$D_{Me^{z+}}$ and D_{tracer} should thus also be measured. This can be achieved either by chronopotentiometry on a stationary electrode, or be measuring the diffusion limiting current density on a rotating disc electrode. By the first method, provided a current density much higher than the diffusion limiting current density is applied to the cell, a transition time, τ, may be measured, for instance according to the method of Besson and Guiton [24], and provided Sand's law for diffusion-controlled processes is verified ($J\tau^{1/2}$ must be constant as a function of J),

$$D = \frac{4 \times 10^{-6}J^2\tau}{\pi z^2F^2C_b} \qquad (7)$$

This formula is valid for Me^{z+} as well as for the tracer, with J in mA cm^{-2} and τ in s.

By the second method, the Levich equation

$$J_{dl} = 0.62 \times 10^{-3}zFD^{2/3}\nu^{-1/6}\omega^{1/2}C_b \qquad (8)$$

allows the calculation of D, where ω is in rad s^{-1}.

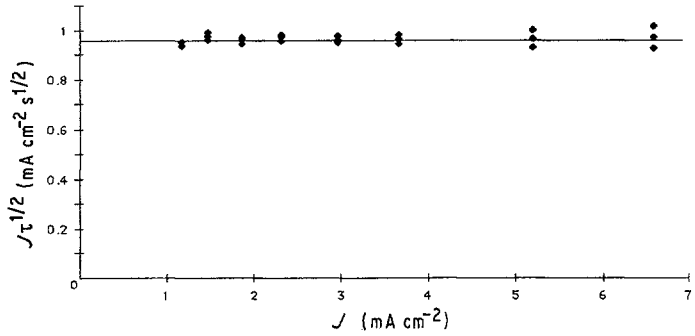

Fig. 2. Validity of Sand equation for silver. Laboratory flow-through channel cell. Electrolyte: 50 g l^{-1} Cu^{2+}, 100 g l^{-1} H_2SO_4, 0.324 g l^{-1} Ag^+, 50° C.

Both methods are generally satisfactory in determining D_{tracer}, because the tracer concentration is low and does not result in a noticeable change in surface area or roughness during the measurement. However, erratic results are sometimes obtained for $D_{Me^{z+}}$, especially when hydrogen evolution occurs.

In the case of fully developed forced laminar flow in a channel cell, Pickett *et al.* [25] and Rousar *et al* [26] have proposed this relationship:

$$Sh \propto Re^{1/3} Sc^{1/3} \tag{9}$$

But, following Eckert [47] who studied a laminar developing flow,

$$Sh \propto Re^{1/2} Sc^{1/3} f(H/H + L) \tag{10}$$

where H is the hydrodynamic entrance length and L is the electrode length.

In the case of laminar natural convection, as may be expected in a copper electrolytic cell, Wilke *et al.* [27] proposed the correlation

$$Sh = 0.66(GrSc)^{1/4} \tag{11}$$

where

$$Gr = gL^3(\varrho_b - \varrho_i)/\varrho\nu^2$$

For turbulent natural convection at a vertical plane, this equation becomes [28–30]

$$Sh = 0.116(GrSc)^{1/3}$$

or more generally

$$Sh \propto (GrSc)^{1/3}$$

It should be noticed that, according to the different types of equations, if in Equation 6 the ratio $D_{Me^{z+}}/D_{\text{tracer}}$ appears to the power 2/3, this power becomes 3/4 only in the case of a laminar natural convection flow.

Recently [32] it was shown that the direct measurement of $J_{\text{dl tracer}}$ was possible by drawing a potentiodynamac cathodic polarization curve restricted to the field of potential where only the tracer may be deposited. Equation 6 is, however, still valid, taking into account the above-mentiond remark concerning the power for $D_{Me^{z+}}/D_{\text{tracer}}$.

Finally, results may be expressed in terms of values of $J_{\text{dl Me}}$, $\delta_{Me^{z+}}$ or of the mass transfer coefficient $k = J_{\text{dl}}/zFC$. Using k values, the Sherwood number is then calculated as $Sh = 10^{-3} kd/D$.

3. Experimental procedure and results

3.1. *Copper sulfate solutions*

A complete study was made for copper deposition in channel cells with forced turbulent flow at laboratory scale [20, 21] and at pilot scale [9]. In the first case, two different cell cross sections were used: 1.6 × 1.5 cm^2 (cell I) and 1.8 × 0.6 cm^2 (cell II). Transient time measurements were made for silver used as the tracer as well as for copper, at 50° C, in a solution containing 50 g l^{-1} Cu^{2+} and 100 g l^{-1} H_2SO_4, and some Ag^+ added as Ag_2SO_4. Figures 2 and 3 show that Sand's law was satisfied in both cases. For the silver measurements anode and cathode were made of silver; for copper both electrodes were copper.

Diffusion coefficients were calculated according to Equation 2:

$$D_{Ag^+} = 1.41 \times 10^{-5} \text{ cm}^2 \text{ s}^{-1}$$

$$D_{Cu^{2+}} = 0.95 \times 10^{-5} \text{ cm}^2 \text{ s}^{-1}$$

Table 1 gives the final results.

Chilton–Colburn's law was also verified in cell I (see Fig. 4), showing that mass transfer was effectively controlled by diffusion and that turbulent flow was achieved even with the lowest value of Re. For a

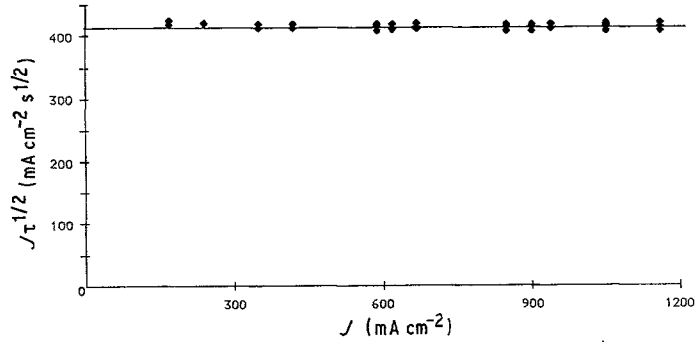

Fig. 3. Validity of Sand equation for copper. Laboratory flow-through channel cell. Electrolyte: 50 g l^{-1} Cu^{2+}, 100 g l^{-1} H_2SO_4, 50° C.

Table 1. Mass transfer in laboratory flow through channel cells

Cell	d (cm)	v ($cm\,s^{-1}$)	Re	$J_{dl\,Ag+}$ ($mA\,cm^{-2}$)	$J_{dl\,Cu2+}$ ($mA\,cm^{-2}$)	$k_{Cu2+} \times 10^2$ ($cm\,s^{-1}$)	δ_{Cu2+} (μm)
I	1.55	56	10610	0.145	950	0.625	15.2
I	1.55	92	17432	0.235	1480	0.974	9.8
I	1.55	135	25579	0.314	2090	1.376	6.9
I	1.55	202	38274	0.451	3000	1.975	4.8
II	0.90	480	52876	0.728	4560	3.003	3.2

Electrolyte 50 $g\,l^{-1}$ Cu^{2+} (0.79 M), 100 $g\,l^{-1}$ H_2SO_4 (1 M), 0.018 $g\,l^{-1}$ Ag^+ (1.67×10^{-4} M), 50° C

Reynolds number of 53 000, the mass transfer coefficient obtained in cell II is higher by 15% than the value expected from the law verified in cell I. This fact shows that care must be taken when extrapolating the results obtained in one cell to another if the Reynolds number is calculated with the hydraulic diameter of the cross section of the cell.

Table 1 shows that very high diffusion-limiting current densities may be achieved and, accordingly, a high current density electrorefining process was studied [9] at pilot scale. The cell was 100 cm long and its section was $20 \times 1.5\,cm^2$. A hydrodynamic study showed that the characteristic hydraulic length to use in Reynolds calculation was 6.4 cm. Making use of an electrolyte containing 40 $g\,l^{-1}$ Cu^{2+} and 174 $g\,l^{-1}$ H_2SO_4 at 60° C, results were obtained as shown in Table 2.

For lower current densities, more in the range encountered in conventional electrowinning or electrorefining (about 20 $mA\,cm^{-2}$), three different experimental set-ups were tested.

(a) A small conventional laboratory cell (a beaker with two small vertical copper electrodes) [48, 49], with a rotating stirrer and of the same tracer method as above, was used to test the influence of organic additives on the diffusion limiting current density at 60° C, in a solution containing 37 $g\,l^{-1}$ Cu^{2+} and 192 $g\,l^{-1}$ H_2SO_4. Table 3 gives the results at constant stirrer rotation speed.

Despite the fact that $D_{Cu^{2+}}$ remained unchanged for all the solutions tested and that the initial roughness of the electrodes was the same for each experiment (due to a 40 μm predeposit made at 40 $mA\,cm^{-2}$ in a pure solution containing no additive), there is a substantial influence of cysteine and of gelatin on $J_{dl\,Cu^{2+}}$. Surprisingly enough, especially for gelatin, an increase of $J_{dl\,Cu^{2+}}$ is observed in the presence of these organic additives. No satisfactory explanation has been given so far.

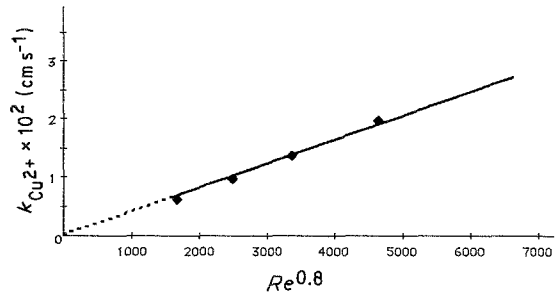

Fig. 4. Validity of Chilton–Colburn equation for copper in channel cell I. Electrolyte: 50 $g\,l^{-1}$ Cu^{2+}, 100 $g\,l^{-1}$ H_2SO_4, 0.018 $g\,l^{-1}$ Ag^+, 50° C.

(b) A large laboratory cell included in a circuit intended to simulate conventional Metallurgie Hoboken-Overpelt industrial copper electrorefining conditions [31]: two copper electrodes 100 cm high and 20 cm large were suspended in a cell at a separation distance of 3 cm, with lateral and bottom spacings to allow natural convection to occur as in industrial cells. Measurements were made according to the codeposition method already described, in a 40 $g\,l^{-1}$ Cu^{2+}, 180 $g\,l^{-1}$ H_2SO_4 electrolyte at 60° C.

It was very difficult to obtain reproducible results making use of silver as tracer as is was quickly precipitated as a very fine metallic powder. O'Keefe *et al.* [32] suggested that this could be due to a reaction between Cu^+ and Ag^+, and accordingly it was decided to add some H_2O_2 to the solution to raise the redox potential. Good results were then obtained giving the following value:

$$J_{dl\,Cu^{2+}} \approx 85\,mA\,cm^{-2} (k_{Cu^{2+}} \approx 0.7 \times 10^{-3}\,cm\,s^{-1})$$

In the same solution but in forced laminar flow in a channel cell with the same distance between the electrodes [33], measurements made with the codeposition method have shown that Eckert's law was verified (see Fig. 5). It is interesting to note that a linear flow velocity of 3 $cm\,s^{-1}$ in the channel cell provides the same mass transfer coefficient as that obtained by natural convection.

(c) Making use of a rotating disc electrode, a modification of Ettel *et al.'s* tracer technique was developed [32] for determining mass transfer coefficients in electrolytes for both copper electrowinning and electrorefining systems. The method involves the direct measurement of the limiting current density of the tracer by cyclic voltammetry in the potential range where only the tracer may be deposited. A Levich

Table 2. Mass transfer in pilot scale flow through electrorefining channel cell

v ($cm\,s^{-1}$)	Re	$J_{dl\,Cu2+}$ ($mA\,cm^{-2}$)	$k_{Cu2+} \times 10^2$ ($cm\,s^{-1}$)	δ_{Cu2+} (μm)
125	80000	2460 ± 300	2.03 ± 0.25	6.0
240	153000	4550 ± 230	3.75 ± 0.19	3.2

Electrolyte 40 $g\,l^{-1}$ Cu^{2+} (0.63 M), 174 $g\,l^{-1}$ H_2SO_4 (1.77 M), 60° C, silver as tracer.

Table 3. Influence of organic additives on the diffusion-limiting current density of copper — conventional laboratory cell

Solution	$J_{dl\,Cu2+}$ ($mA\,cm^{-2}$)	$k_{Cu2+} \times 10^3$ ($cm\,s^{-1}$)	δ_{Cu2+} (μm)
No additive	94 ± 2	0.84 ± 0.02	143
4.1×10^{-5} M cysteine	129 ± 4	1.15 ± 0.04	104
8.2×10^{-5} M cysteine	139 ± 6	1.24 ± 0.05	97
4.1×10^{-5} M tyrosine	100 ± 15	0.89 ± 0.13	135
8.2×10^{-5} M tyrosine	100 ± 15	0.89 ± 0.13	135
3 mg l^{-1} gelatin ASF	119 ± 8	1.06 ± 0.07	113
10 mg l^{-1} gelatin ASF	160 ± 10	1.42 ± 0.09	85

Electrolyte: 37 g l^{-1} Cu^{2+} (0.58 M), 192 g l^{-1} H_2SO_4 (1.96 M), 60° C.

Table 4. Silver mass transfer coefficient and diffusion layer thickness on an RDE

rpm	$\omega^{1/2}$ ($s^{-1/2}$)	J_{dl}/C_{Ag+} ($A\,cm\,g^{-1}$)	$k_{Ag+} \times 10^3$ ($cm\,s^{-1}$)	δ_{Ag+} (μm)
400	6.47	4200	4.70	26.1
900	9.71	6200	6.93	17.7
1600	12.94	8200	9.17	13.4
2500	16.18	10200	11.40	10.7

25 g l^{-1} Cu^{2+} (0.39 M), 100 g l^{-1} H_2SO_4 (1 M), 0.015 g l^{-1} Ag^+ (1.39×10^{-4} M) solution at 23° C. $D_{Ag+} = 1.22 \times 10^{-5}\,cm^2\,s^{-1}$; $\nu = 0.0117\,cm^2\,s^{-1}$; electrode radius = 0.564 cm.

plot was obtained on a platinum electrode in a 25 g l^{-1} Cu^{2+}, 100 g l^{-1} H_2SO_4, 0.01 g l^{-1} Ag^+ electrolyte, at 23° C (see Fig. 6), showing that the process was diffusion controlled. Values in the range of 1.12 to $1.23 \times 10^{-5}\,cm^2\,s^{-1}$ were obtained for D_{Ag+}.

Table 4 gives value of the mass transfer coefficient and of the diffusion layer thickness for various rotation speeds of the electrode. The highest Reynolds number estimated for 2500 rpm was 34 960, and is below the limit for the onset of turbulent flow which, for a well centered electrode, occurs at about [34] $Re_{cr} = 2 \times 10^5$. The mass transfer coefficient for copper was calculated by

$$k_{Cu^{2+}} = k_{Ag^+}\left(\frac{D_{Cu^{2+}}}{D_{Ag^+}}\right)^{2/3} \qquad (12)$$

making use of a value for $D_{Cu^{2+}}$ calculated from the expression [35, 36]

$$D_{Cu^{2+}\,18°C} = 4.7 \times 10^{-5}/(5.0 + \Gamma) \qquad (13)$$

where Γ is the ionic strength. For a 100 g l^{-1} H_2SO_4, 25 g l^{-1} Cu^{2+} solution, $D_{Cu^{2+}}$ is $0.488 \times 10^{-5}\,cm^2\,s^{-1}$ and D_{Ag^+} is $1.22 \times 10^{-5}\,cm^2\,s^{-1}$. At 400 rpm, $k_{Ag+} = 4.7 \times 10^{-3}\,cm\,s^{-1}$ as given in Table 4 and accordingly $k_{Cu^{2+}} = 2.54 \times 10^{-3}\,cm\,s^{-1}$.

Problems were encountered when $C_{Cu^{2+}}$ and temperature increased. The diffusion coefficient, D_{Ag^+}, calculated on the basis of chemical analysis of copper and silver codeposits, gave values about three times greater than those obtained when only silver was deposited. Moreover, it was found that silver had also deposited on the nonworking area of the RDE, suggesting as a possible cause a redox reaction of the type

$$Ag^+ + Cu^+ \longrightarrow Ag + Cu^{2+} \qquad (14)$$

The previously mentioned experiments in a large electrorefining cell, where it was necessary to raise the redox potential by adding H_2O_2 to the solution, give support to this idea.

It should be interesting to re-evaluate the influence of organic additives on the diffusion-limiting current density described in the previous paragraph using this method.

3.2. *Zinc sulfate solutions*

A laboratory-scale study [37] was also made in channel cells with forced turbulent flow, resulting in the development of large pilot-scale industrial equipment [38, 39].

Making use of a solution containing 80 g l^{-1} Zn^{2+}, 135 g l^{-1} H_2SO_4 at 50° C, with Cd^{2+} as tracer, the diffusion limiting current density for Zn^{2+} was determined by the codeposition method as shown in Table 5.

Current efficiency for zinc deposition was always high, so that hydrogen evolution was proportionally rather low. Nevertheless, $k_{Zn^{2+}}$ values depended on the codeposition current density, especially at low electrolyte velocities; thus the Chilton–Colburn equation is not verified.

The influence of hydrogen evolution appears in a more striking way in the case of Zn–Fe alloys [44], where current efficiencies may be low (50–70%). The same codeposition technique was used in a channel cell including a diaphragm to separate anolyte from catholyte in order to avoid any influence of Fe^{3+} reduction at the cathode for electrolytes with various metal concentrations. In this case, the contribution of hydrogen evolution to mass transfer could be evaluated quantitatively, considering that the diffusion

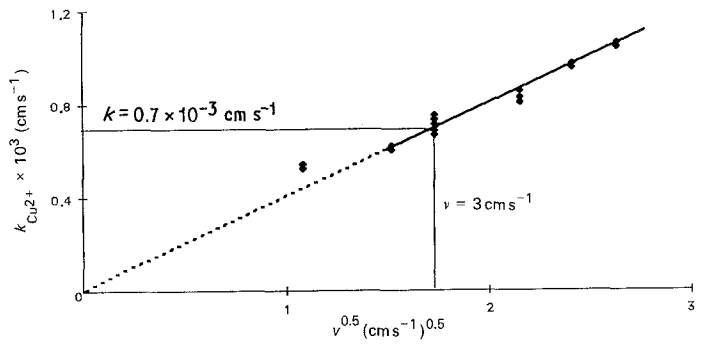

Fig. 5. Validity of Eckert equation for copper in forced laminar flow in a channel cell. Electrolyte: 40 g l^{-1} Cu^{2+}, 180 g l^{-1} H_2SO_4, 60° C, silver as tracer.

Table 5. Mass transfer in laboratory flow through channel cell

v ($cm\,s^{-1}$)	Re	J ($mA\,cm^{-2}$)	r_c (%)	$J_{dl\,Zn2+}$ ($mA\,cm^{-2}$)	$k_{Zn2+} \times 10^3$ ($cm\,s^{-1}$)	δ_{Zn2+} (μm)
100	11 220	500	94	1986	8.41	11.9
		1000	92	2110	8.93	11.2
		1500	87	2371	10.04	10.0
200	22 440	500	92	3356	14.21	7.0
		1000	94	3356	14.21	7.0
		1500	94	3466	14.68	6.8
300	33 660	500	90	4401	18.64	5.4
		1000	95	4594	19.45	5.1
		1500	96	4511	19.10	5.2
400	44 880	500	92	5639	23.88	4.2
		1000	96	5474	23.18	4.3
		1500	96	5777	24.46	4.1

Electrolyte: $80\,g\,l^{-1}$ Zn^{2+} (1.22 M), $135\,g\,l^{-1}$ H_2SO_4 (1.38 M), $5\,mg\,l^{-1}$ Cd^{2+} (4.45×10^{-5} M), 50° C.

limiting current density or, better, the mass transfer coefficient contains two additive parts [40, 41]. One contribution is due to macroconvection (forced flow of the electrolyte) with k_v proportional to $v^{0.8}$ according to the Chilton-Colburn equation, and the other is due to microconvection (intense local agitation in the diffusion layer due to gas bubbling through it) with k_g proportional to the square root [42, 43] of the partial current density for hydrogen evolution J_{H_2}. Figure 7 shows the results obtained at $200\,cm\,s^{-1}$, 50° C in sulfate electrolytes containing H_2SO_4 0.2 M, $10\,mg\,l^{-1}$ Cd^{2+} and various amounts of Fe^{2+} and Zn^{2+} between 0.75 and 1 M for Fe^{2+} and 0.1–0.75 M for Zn^{2+} as indicated in the figure. As can be seen, the partial mass transfer coefficient for zinc due to macroconvection is in the range of $0.67 \times 10^{-2}\,cm\,s^{-1}$, and that value may be increased by 50% if the partial current density for hydrogen reaches about $500\,mA\,cm^{-2}$, which is already high. Results in Fig. 7 may be expressed as follows (J is in $mA\,cm^{-2}$):

$$k_{Zn^{2+}} = 0.67 \times 10^{-2} + 0.16 \times 10^{-3} J_{h_2}^{1/2} \quad (15)$$

For other flow rates, we may take away from the total mass transfer coefficient for zinc the part due to the hydrogen evolution calculated by Equation 15. The mass transfer coefficient due to macroconvection versus the flow velocity exponent 0.8 is plotted in Fig. 8 and a straight line indicates that the Chilton–Colburn relation is verified:

$$k_{v\,Zn^{2+}} = 0.97 \times 10^{-4} v^{0.8} \text{ (where } v \text{ is in cm s}^{-1}\text{)} \quad (16)$$

With the same procedure applied to the results of Table 5, a similar contribution of hydrogen evolution to mass transfer was found to be:

$$k_{g\,Zn^{2+}} = 0.18 \times 10^{-3} J_{H_2}^{1/2} \quad (17)$$

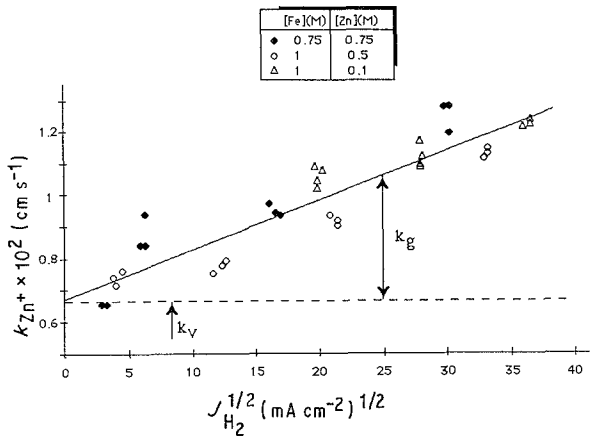

Fig. 7. Relation between the mass transfer coefficient for zinc and the square root of the hydrogen partial current density. Zn–Fe sulfate electrolytes: 0.2 mole l^{-1} H_2SO_4, 50° C, $v = 2\,m\,s^{-1}$, Zn^{2+} and Fe^{2+} as indicated.

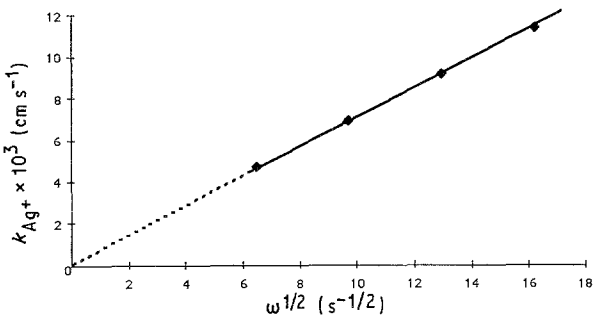

Fig. 6. Levich plot for silver deposited on a rotating disc Pt electrode. Electrolyte: $25\,g\,l^{-1}$ Cu^{2+}, $100\,g\,l^{-1}$ H_2SO_4, $0.01\,g\,l^{-1}$ Ag^+, 23° C.

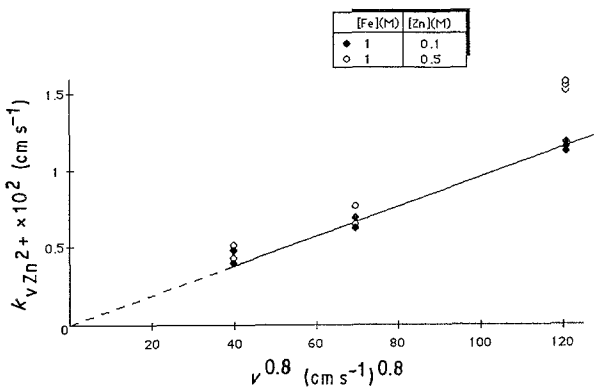

Fig. 8. Relation between the mass transfer coefficient for zinc due to macroconvection and the electrolyte flow rate. Zn–Fe sulfate electrolytes: 0.2 mole l^{-1} H_2SO_4, 50° C, Zn^{2+} and Fe^{2+} as indicated.

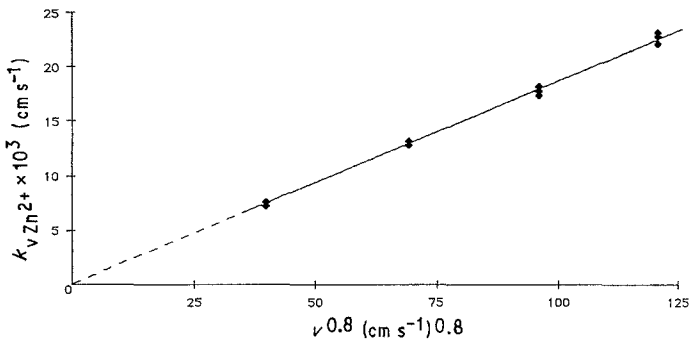

Fig. 9. Validity of Chilton-Colburn equation for zinc in channel cell II. Electrolyte: 80 g l^{-1} Zn^{2+}, 135 g l^{-1} H_2SO_4, 50° C, 5 mg l^{-1} Ag^+ as tracer.

After subtracting the gas evolution portion of the total mass transfer coefficient for zinc, the Chilton–Colburn relationship is then verified (Fig. 9):

$$k_{v\,Zn^{2+}} = 0.186 \times 10^{-3} v^{0.8} \quad (18)$$

Independent experiments were performed [45] in a vertical flow-through laboratory scale channel cell ($d_{A/C}$ = 0.9 cm) with silver as tracer. The potentiodynamic method was used to characterize $J_{dl\,Ag^+}$ alone in the potential range where only silver can be deposited, without zinc deposition and also without hydrogen evolution. Under the same flow rate conditions, a Zn–Ag codeposit was produced at 100 mA cm^{-2}, and the new values were calculated for zinc mass transfer to the electrode by chemical analysis. For potentiodynamic measurements, both electrodes were made of silver, whereas low carbon steel was the cathode and either zinc or lead the anode for Zn–Ag codeposition. Table 6 shows the values obtained by the potentiodynamic method, and Table 7 gives those obtained by the codeposition method.

Comparing the values of Tables 6 and 7, it can be seen that hydrogen evolution gives a noticeable enhancement in mass transfer ($k_{g\,Zn^{2+}} \approx 0.37 \times 10^{-3} J_{H_2}^{1/2}$), whereas oxygen evolution at the anode does not result in a further enhancement, at least at that scale and with this small distance between the electrodes. Figure 10 shows that a plot of $k_{Zn^{2+}}$ values from Table 6 versus $v^{0.8}$ is in agreement with the Chilton–Colburn equation for turbulent flow.

For lower current densities, in the range encountered in conventional electrowinning cells (about 40 mA cm^{-2}), three different experimental set-ups were tested:

(a) In a small beaker cell (400 ml), 1 cm^2 vertical strip electrodes were placed [45]. The limiting current density of the silver tracer was measured by cyclic voltammetry in the potential range where only silver can be deposited, making use of Pt electodes, in a 100 g l^{-1} Zn^{2+}, 0.017 g l^{-1} Ag^+ sulfate electrolyte at pH 1.5. $J_{dl\,Ag^+}$ was also measured by the codeposition method making use of low carbon steel as the cathode

Table 6. Mass transfer data obtained by the potentiodynamic method

	Flow rate (cm s^{-1})				
	0	*50*	*100*	*200*	*300*
$J_{dl\,Ag^+}$ (mA cm^{-2})	0.0034	0.070	0.118	0.195	0.270
$k_{Ag^+} \times 10^3$ (cm s^{-1})	0.51	10.6	17.8	29.5	40.8
$k_{Zn^{2+}} \times 10^3$ (cm s^{-1})	0.42	8.80	14.8	24.5	33.9
$J_{dl\,Zn^{2+}}$ (mA cm^{-2})	159	3329	5600	9269	12826
δ (μm)	214	10	6.1	3.7	2.7

Laboratory flow-through channel cell. Electrolyte 100 g l^{-1} Zn^{2+} (1.53 M), pH 1.5 by H_2SO_4, 6 mg l^{-1} (5.56 × 10^{-5} M) Ag^+ as tracer, 60° C.

Table 7. Mass transfer data obtained by the codeposition method

Plating conditions	*Zn anode*				*Pb anode*			
	Stationary		*100 cm s^{-1}*		*Stationary*		*100 cm s^{-1}*	
	U	*L*	*U*	*L*	*U*	*L*	*U*	*L*
$J_{dl\,Ag^+}$ (mA cm^{-2})	0.111	0.101	0.146	0.180	0.082	0.059	0.145	0.170
$k_{Ag^+} \times 10^3$ (cm s^{-1})	17.5	15.9	23.0	28.3	12.9	9.29	22.8	27.0
$k_{Zn^{2+}} \times 10^3$ (cm s^{-1})	14.5	13.2	19.2	23.5	10.7	7.71	19.0	22.5
$J_{dl\,Zn^{2+}}$ (mA cm^{-2})	5490	4994	7219	8902	4056	2917	7173	8500
δ (μm)	6.2	6.8	4.7	3.8	8.4	11.7	4.8	4.0
r_c (%)	84	75	84	88	76	83	89	93

Laboratory flow-through channel cell. Electrolyte 100 g l^{-1} Zn^{2+} (1.53 M), pH 1.5 by H_2SO_4, 6 mg l^{-1} (5.56 × 10^{-5} M) Ag^+ as tracer, 60° C.
U = upper half of electrode; L = lower half.

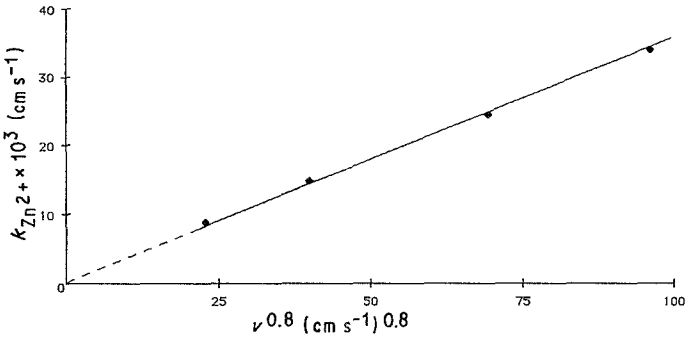

Fig. 10. Mass transfer coefficient for zinc values from Table 6 against $v^{0.8}$. Electrolyte: 100 g l^{-1} Zn^{2+}, pH 1.5 by H_2SO_4, 60° C, 6 mg l^{-1} Ag^+ as tracer.

and zinc as the anode. Results are shown in Table 8 for various types of agitation.

In this case, at least for the stationary electrolyte, the hydrogen evolution enhancement mass transfer was very important, resulting in an increase by a factor of 10 for $k_{Zn^{2+}}$. This value is due to a J_{H_2} of 10 mA cm^{-2} ($r_c \approx 93\%$).

(b) In the same small beaker cell, the potentiodynamic method was used in the range where only silver was deposited on the platinum rotating disc-electrode. Table 9 gives the results.

(c) In a large laboratory cell included in a circuit intended to simulate conventional Super Jumbo Vieille Montagne industrial conditions [46]. This consisted of one lead–silver anode and one aluminium starting sheet cathode 165 cm high and 20 cm large suspended in a cell at a distance of 3 cm from one another, with lateral and bottom spacings allowing natural convection to occur as in industrial cells. Measurements were made according to the codeposition method at 40 mA cm^{-2} in a 50 g l^{-1} Zn^{2+}, 180 g l^{-1} H_2SO_4 electrolyte at 35° C, making use of Cd^{2+} (10 mg l^{-1}) as tracer. Values around 90 mA cm^{-2} were obtained for $J_{dl\,Zn^{2+}}$ or 0.61×10^{-3} cm s^{-1} for $k_{Zn^{2+}}$. These results were confirmed in actual industrial cells, making use of existing concentrations of Cd^{2+} and Cu^{2+} as tracers. Due to the high value of current efficiency (92%) and the lower value of current density (40 mA cm^{-2} instead of 150 mA cm^{-2} — Table 8), the influence of hydrogen evolution is smaller. To compare these results with those from Table 8, the ratio of the two mass transfer coefficients is equal to the square root of the ratio of the two codeposition current densities. However, as can be expected for these natural convection cells, diffusion limiting current densities change along the height of the electrodes, from 65 mA cm^{-2} near the bottom to about 92 mA cm^{-2} in the large laboratory cell and from 74 mA cm^{-2} to 105 mA cm^{-2} in industrial cells.

In the same solution but in forced laminar flow in a channel cell with the same distance between the electrodes, measurements made with the codeposition method have shown that Eckert's law was verified (see Fig. 11). A linear flow velocity of 8.3 cm s^{-1} in the channel cell provides the same mass transfer coefficient as that obtained by natural convection.

4. Conclusion

Mass transfer measurements by the tracer technique give consistent and reproducible results, provided a certain number of rules are observed. These include checking for true diffusion control, determining the type of hydrodynamic flow and ensuring that no side reaction occurs leading to consumption of the tracer.

The potentiodynamic method was used to measure the tracer diffusion limiting current density and the calculated $J_{dl\,Me}$ were compared with values obtained from codeposition measurements. The results were very similar and, in addition, the potentiodynamic techniques proved to be an excellent tool to investigate separately mass transfer due to macroconvection and the enhancement of this due to hydrogen evolution. Results obtained by this method and by another

Table 8. Comparison of mass transfer properties obtained by potentiodynamic measurement and codeposition method — small beaker cell with vertical electrodes

	Potentiodynamic measurement				*Zn-Ag codeposition at 150 mA cm^{-2}*			
	$k_{Ag+} \times 10^3$ (cm s^{-1})	$k_{Zn2+} \times 10^3$ øø(cm s^{-1})	$J_{dl\,Zn2+}$ (mA cm^{-2})	δ_{Zn2+} (μm)	$k_{Ag+} \times 10^3$ (cm s^{-1})	$k_{Zn2+} \times 10^3$ (cm s^{-1})	$J_{dl\,Zn2+}$ (mA cm^{-2})	δ_{Zn2+} (μm)
Stationary electrolyte	0.18	0.11	42	341	1.90	1.18	446	32
Electrolyte flow	2.24	1.39	526	27	3.46	2.14	813	18
N_2 sparging (26 cm^3 min^{-1})	2.30	1.42	540	27	3.61	2.24	848	17
Ultrasonic vibration	0.99 to 6.58	0.61 to 4.07	233 to 1546	62 to 9	4.95	3.06	1163	12
Brushing	6.25	3.87	1469	10	7.48	4.63	1758	8

Electrolyte: 100 g l^{-1} Zn^{2+} (1.53 M), 0.017 g l^{-1} Ag^+ (1.58×10^{-4} M), pH: 1.5; 60° C.

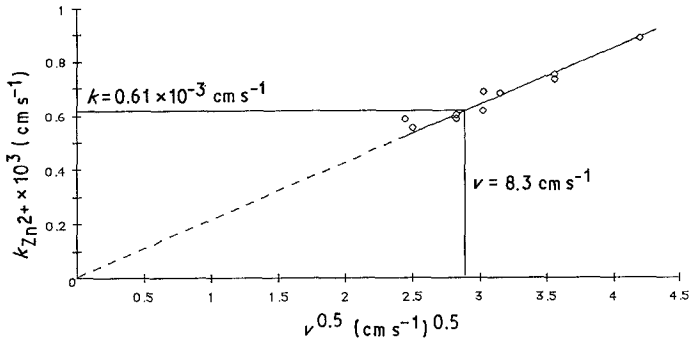

Fig. 11. Validity of Eckert equation for zinc in forced laminar flow in channel cell. Electrolyte: 50 g l^{-1} Zn^{2+}, 180 g l^{-1} H_2SO_4, 35° C, 10 mg l^{-1} Cd^{2+} as tracer.

Table 9. Mass transfer parameters measured by potentiodynamic method on a Pt rotating disc electrode

rpm	$J_{dl\,Ag+}$ (mA cm^{-2})	$k_{Ag+} \times 10^3$ (cm s^{-1})	$J_{dl\,Zn2+}$ (mA cm^{-2})	$k_{Zn2+} \times 10^3$ (cm s^{-1})	δ_{Zn2+} (μm)
400	0.065	3.60	1108	2.01	20.3
2500	0.167	9.26	2845	5.16	7.9

Electrolyte: 155 g l^{-1} Zn^{2+} (2.37 M), 0.02 g l^{-1} Ag^+ (1.85×10^{-4} M), pH 4; 60° C $D_{Ag+} = 9.91 \times 10^{-6}$ cm^2 s^{-1}.

independent method show that this enhancement from gas evolution may be important, especially at high current density and with low cathode current efficiency.

High mass transfer can be achieved in flow-through channel cells as already applied in industry, especially for continuous coil plating. Nevertheless, to improve the use of these mass transfer measurements, especially to extrapolate the results obtained in laboratory flow-through channel cells to industrial cells, it is necessary to find a method to determine the hydraulic length characteristic of all the cell cross section types.

References

[1] H. Fischer, Elektrolytische Abscheidung und Elektrokristallisation von Metallen Springer, Berlin (1965).
[2] R. Winand, *Mém. Scient. Revue Métall.* **58** (1961) 25.
[3] R. Winand, *Trans. IMM Sect. C* **84** (1975) 67.
[4] R. Winand, in 'Application of Polarization Measurements in the Control of Metal Deposition (edited by I. H. Warren), Elsevier, Amsterdam (1984) pp. 47–83.
[5] M. Lambert and R. Winand, *Oberfläche/Surface* **8** (1977) 208.
[6] W. W. Harvey, in 'Energy Reduction Techniques in Metal Electrochemical Processes' (edited by R. G. Bautista and R. T. Wesely), TMS – AIME (1980) pp. 93–110.
[7] K. A. Spring and J. W. Evans, *ibid.*, pp. 309–318.
[8] Third, Fourth and Fifth Meetings of the American Electroplaters Society on Continuous Strip Plating – respectively Annapolis, April 1980, Chicago, May 1984, Detroit, May 1987.
[9] Ph. Harlet and R. Winand, in 'Electrowinning and Electrorefining of Copper' (edited by J. E. Hoffmann, R. G. Bautista, V. A. Ettel, V. Kudryk and R. J. Wesely), TMS – AIME (1987) pp. 239–267.
[10] J. R. Lloyd, E. M. Sparrow and E. R. Eckert, *J. Electrochem. Soc.* **119** (1972) 702.
[11] G. Wranglen and O. Nilson, *Electrochim. Acta* 7 (1962) 121.
[12] N. Ibl, *Chemie Ing. Tech.* **43** (1971) 202.
[13] A. Tvarusko and L. S. Watkins *Electrochim. Acta* **14** (1969) 1109.
[14] A. Tvarusko and L. S. Watkins, *J. Electrochem. Soc.* **118** (1971) 580.
[15] F. R. McLarnon, R. H. Muller and W. C. Tobias, *Electrochim. Acta* **21** (1976) 101.
[16] Y. Awakura and Y. Konda, *J. Electrochem. Soc.* **123** (1976) 8, 1184.
[17] Y. Awakura, Y. Takenaka and Y. Kondo, *Electrochim. Acta* **21** (1976) 789.
[18] A. Brenner, *Proc. Am. Electroplat. Soc.* **95** (1940) 4.
[19] V. A. Ettel, B. V. Tilak and A. S. Gendron, *J. Electrochem. Soc.* **121** (1974) 7, 867.
[20] M. Degrez and R. Winand, *Revue ATB Met.* **19** (1979) 21.
[21] M. Degrez and R. Winand *Electrochim. Acta* **29** (1984) 365.
[22] T. J. O'Keefe, J. S. Cuzmar and S. F. Chen, Evaluation of mass transfer coefficients in metal deposition by electrochemical techniques. Paper presented at the 115th AIME Annual Meeting, New Orleans, LA, March 1986.
[23] D. J. Pickett and K. Ong, *Electrochim. Acta* **19** (1974) 875.
[24] J. Besson and J. Guitton, *J. Chim. Phys.* **67** (1970) 1097.
[25] D. J. Pickett and B. R. Stanmore, *J. Appl. Electrochem.* **2** (1972) 151.
[26] I. Rousar, J. Hostomsky, V. Cesner and B. Stverak, *J. Electrochem. Soc.* **118** (1971).
[27] C. R. Wilke, C. W. Tobias and M. Eisenberg, *Chem. Eng. Progr.* **49** (1953) 663.
[28] A. A. Wragg, *Electrochim. Acta* **13** (1968) 2159.
[29] E. J. Fenech and C. W. Tobias, *Electrochim. Acta.* **2** (1960) 311.
[30] N. Ibl, *Electrochim. Acta.* **24** (1979) 1105.
[31] V. Bastin, M. Degrez and R. Winand, Restricted report to Metallurgie Hoboken Overpelt, ULB (1987).
[32] T. J. O'Keefe, J. S. Cuzmar and S. F. Chen, *J. Electrochem. Soc.* **134** (1987) 547.
[33] B. Tshula-Kabongo, Electrorefining of copper. PhD Thesis, ULB (1983).
[34] A. J. Bard and L. R. Faulkner, 'Electrochemical Methods. Fundamentals and Applications', John Wiley, New York (1980).
[35] S. Bruckenstein, J. W. Sharkey and J. Y. Yip, *Anal. Chem.* **57** (1985) 368.
[36] P. Hannaert, *Ind. Chim. Belge,* **32** (1967) 223.
[37] A. Weymeersch, R. Winand and L. Renard, Plating and Surface Finishing, April (1981), pp. 56-59.
[38] R. Winand, *Oberfläche/Surface* **25** (1984) 11.
[39] A. Wymeersch, L. Renard, J. J. Conreur, R. Winand, M. Jorda and C. Pellet, *Plating Surface Finish* **73** (1986) 67.
[40] T. R. Beck, *J. Electrochem. Soc.* **116** (1969) 1038.
[41] M. D. Birkett and A. Kuhn, *Electrochim. Acta* **22** (1977) 1427.
[42] N. Ibel and J. Venczel, *Metalloberfläche* **24** (1970) 365.
[43] J. L. Janssen and J. Hoogland, *Electrochim. Acta* **15** (1970) 1013.
[44] A. Rodriguez Fajardo, R. Winand, A. Weymeersch and L. Renard, Fundamental aspects of Zn–Fe alloys electrodepostion. Fifth AES Continuous Strop Plating Symposium, Detroit, May 1987.
[45] S. F. Chen, J. S. Cuzmar, T. J. O'Keefe, E. R. Cole, V. R. Miller and J. H. Lindsay, Measurements of mass transfer effects in sulfate electrogalvanizing electrolyte. Fifth AES Continuous Strip Plating Symposium, Detroit, May 1987.
[46] M. Degrez and R. Winand, Restricted report to Vieille Montagne, ULB (1987).
[47] E. R. G. Eckert and R. M. Drake, 'Heat and Mass Transfer', McGraw-Hill, New York (1959).
[48] G. Troch, Influence of inhibitors on copper electrodeposition in sulphuric solution. PhD Thesis ULB (1983).
[49] G. Troch, M. Degrez and R. Winand, *Proc. Electrochem. Soc.* **84** (1984) 10, 642.